

# Optical Production of Stable Ultracold $^{88}\text{Sr}_2$ Molecules

G. Reinaudi,<sup>1</sup> C. B. Osborn,<sup>1</sup> M. McDonald,<sup>1</sup> S. Kotochigova,<sup>2</sup> and T. Zelevinsky<sup>1,\*</sup>

<sup>1</sup>*Department of Physics, Columbia University, 538 West 120th Street, New York, NY 10027-5255, USA*

<sup>2</sup>*Department of Physics, Temple University, Philadelphia, PA, 19122, USA*

(Dated: November 24, 2018)

We have produced large samples of ultracold  $^{88}\text{Sr}_2$  molecules in the electronic ground state in an optical lattice. The molecules are bound by  $0.05\text{ cm}^{-1}$  and are stable for several milliseconds. The fast, all-optical method of molecule creation via intercombination line photoassociation relies on a near-unity Franck-Condon factor. The detection uses a weakly bound vibrational level corresponding to a very large dimer. This is the first of two steps needed to create  $\text{Sr}_2$  in the absolute ground quantum state. Lattice-trapped  $\text{Sr}_2$  is of interest to frequency metrology and ultracold chemistry.

PACS numbers: 33.20.-t, 34.50.Rk, 37.10.Jk, 37.10.Pq

The rapid progress of laser cooling has given rise to many new fields of research. One important example is the study of ultracold, dense clouds of molecules. The molecules can exhibit new physical phenomena when brought close to quantum degeneracy [1–3]. For example, long-range anisotropic interactions are expected for heteronuclear polar molecules. Such molecules have also been explored as a paradigm for quantum information and computation [4]. On the other hand, homonuclear molecular dimers without a dipole moment present a metrological interest, for example in constraining the variation of the electron-proton mass ratio [5, 6] or complementing atomic clocks by serving as time standards in the THz regime [6]. Such molecules have also been an excellent testing ground for many possible approaches to creating large ultracold samples, trapping them to allow long interrogation times, and precisely controlling their quantum states. The four promising routes toward trapped neutral molecules [1] are direct control of polar molecule dynamics via electric fields; buffer gas cooling of magnetic species; recent work on direct laser cooling of a suitable class of molecules [7]; and using magnetic or optical fields to combine laser cooled atoms into dimers [8–12]. The latter process tends to result in molecules with relatively small binding energies, but nonetheless has played a major role in the study of new phenomena [13]. These dimers are also most promising for quantum control, since they are typically produced at sub- $\mu\text{K}$  temperatures.

In this Letter, we describe optical production of  $^{88}\text{Sr}_2$  in the electronic ground state in an optical lattice. In contrast to alkali atoms typically used to produce ultracold dimers, Sr atoms possess no electronic spin, and cannot be combined into molecules via the magnetic Feshbach resonance technique [14]. However, Sr has the advantage of the intercombination (spin-forbidden) transition from the ground state,  $^1S_0 - ^3P_1$  (7 kHz line width [15], 689 nm wavelength), which allows Doppler cooling to  $< 1\ \mu\text{K}$  [16], and provides several features that enable efficient photoassociation (PA) into molecules [15, 17]. The unusually fast time scale (0.25 s) for the entire cycle of ultracold molecule production is particularly important

for establishing a short duty cycle in metrological applications. Furthermore, there is active interest in exploring molecules of alkaline earth (and the isoelectronic Yb) atoms in various combinations with each other and with alkalis, such as  $\text{Sr}_2$ ,  $\text{Yb}_2$ ,  $\text{LiYb}$ ,  $\text{RbYb}$ , and  $\text{SrYb}$  [18–24].

Our approach takes advantage of several interesting properties presented by the narrow intercombination transition to achieve efficient transfer of atoms into molecules. Figure 1 (a) and its caption explain the notation used in this work. The excited molecular potential (dissociating to the  $^1S_0 + ^3P_1$  atomic limit) has a small  $C_3$  dispersion coefficient, and a  $C_6$  similar to that of the ground state, resulting in relatively large wave function overlaps with the ground state van der Waals potential [15]. This leads to several Franck-Condon factors (FCFs) between high-lying vibrational states that are unusually close to unity. We exploit these large FCFs for one-photon PA that is followed by spontaneous decay to predominantly a single vibrational quantum state. Another feature enabled by the narrow spectral line is the possibility to frequency resolve the least-bound electronically excited vibrational level with only a  $440\ h\times\text{kHz}$  binding energy corresponding to the dimer size exceeding  $500\ a_0$  [15] ( $h$  is the Planck constant and  $a_0 \approx 0.053\text{ nm}$  is the Bohr radius). This level has an optical length  $l_{\text{opt}}$  (the coupling strength proportional to the PA laser intensity and the free-bound wave function overlap) that is estimated to be  $\sim 10^4$  times larger than for the vibrational levels detuned by 100's of MHz from the dissociation limit. We tune the atom recovery laser to the bound-bound transition resonant with this level, and a significant fraction of the resulting spontaneous decay results in reappearance of ground state atoms. Finally, this molecule creation method is the first step in a two-step process of producing  $\text{Sr}_2$  in the absolute ground quantum state. Recent work [25, 26] predicts large two-photon coupling of the vibrational level  $v = -3$  (Fig. 1) to the absolute ground state  $v = 0$  via an intermediate  $v'$ . We have made the molecules in  $v = -2$  via PA into  $v' = -5$  ( $3.5\ h\times\text{GHz}$  binding energy); however, the calculated and measured FCF is also near unity for  $(v, v') = (-3, -6)$ , and our technique can be used for PA into  $v' = -6$  ( $8.4\ h\times\text{GHz}$

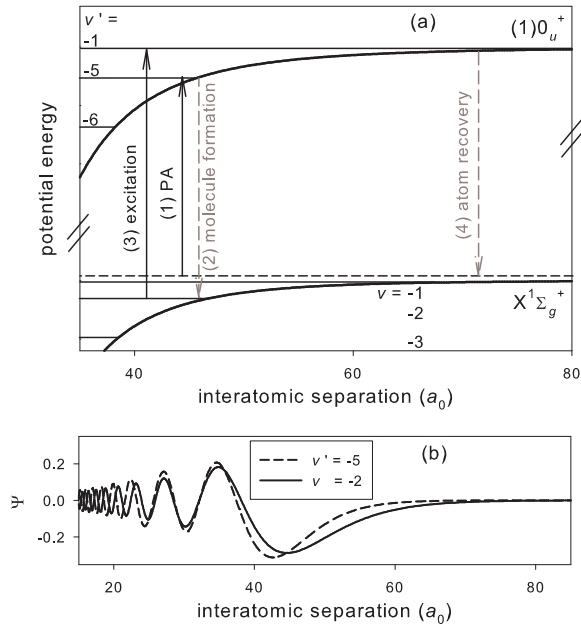


FIG. 1: (a) The long-range  $\text{Sr}_2$  potential energies versus internuclear separation. The two curves relevant to this work are the ground state potential  $X^1\Sigma_g^+$  and the excited state potential  $(1)0_u^+$  that dissociate to the  $^1S_0 + ^1S_0$  and  $^1S_0 + ^3P_1$  atomic limits, respectively. Several vibrational energy levels  $v, v'$  are shown, with the total molecular angular momenta  $(J, J') = (0, 1)$ ; the primed values refer to the excited potential. The negative  $v, v'$  values refer to counting from the dissociation limit, with  $-1$  corresponding to the highest-lying level. The natural line widths of the shown  $v'$  levels are only  $\sim 15$  kHz. The horizontal dashed line indicates the thermal continuum for the  $\mu\text{K}$  atoms. The vertical solid arrows indicate one-photon optical pathways used for molecule creation and atom recovery. The vertical dashed arrows indicate decay pathways completing the molecule creation and recovery; these rely on the unusually large Franck-Condon factor (FCF) and optical length, respectively. (b) The large value of the FCF  $f_{(-2,-5)} \approx 0.8$  results from an excellent agreement of the outer turning points, as illustrated by the wave function plots for these vibrational levels. The theoretical data is courtesy of R. Moszynski, C. Koch, and W. Skomorowski.

binding energy) by attaining a higher power output of the PA laser. Furthermore, theoretical results indicate that two-photon production of  $\text{Sr}_2$  in the absolute ground quantum state from  $v = -2$  should also be feasible, with an efficiency reduced by roughly  $2\times$  [27]. The ability to make deeply bound  $\text{Sr}_2$  can enable a new class of highly precise molecular metrology tools [6].

Producing  $\text{Sr}_2$  in the electronic ground state required performing precise two-photon PA spectroscopy. Our search for  $v = -2$  and  $v = -3$  was guided by the most accurate ground and excited state potentials available from Refs. [28, 29]. Starting with  $5 \times 10^5$   $1\text{-}\mu\text{K}$  Sr atoms trapped in a  $10\text{-}20$   $\mu\text{K}$  deep one-dimensional opti-

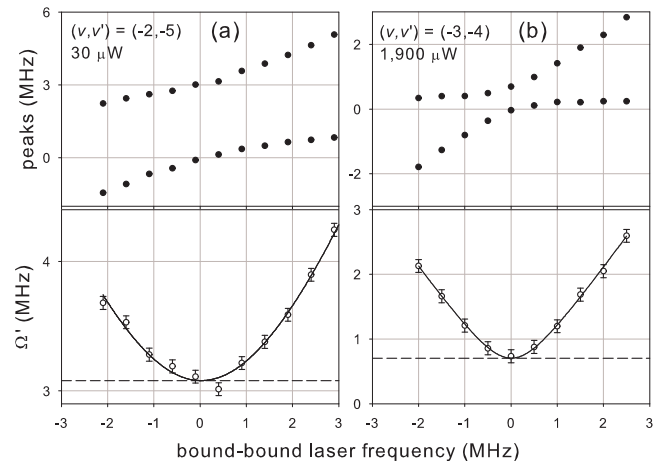


FIG. 2: Autler-Townes doublets emerge when the  $L_{\text{BB}}$  frequency is fixed near a molecular resonance while  $L_{\text{FB}}$  is scanned. (a) Autler-Townes peak positions, along with their separation  $\Omega'$  fitted to eq. (1), for  $(v, v') = (-2, -5)$ . The dashed line indicates the on-resonance Rabi frequency  $\Omega$  at the indicated  $L_{\text{BB}}$  power. (b) Same as (a), for  $(v, v') = (-3, -4)$ . The  $L_{\text{BB}}$  power is  $60\times$  larger, while  $\Omega$  is  $4.4\times$  smaller, resulting in  $f_{(-3,-4)}/f_{(-2,-5)} = 0.9 \times 10^{-3}$ .

cal lattice at  $914$  nm [30], we carried out the spectroscopy via intermediate electronically excited levels, with varying detunings from  $v'$ . The polarizations of all the co-propagating PA and detection lasers in this work are parallel to each other and to the small residual magnetic field at the atom trapping site. When the bound-bound laser ( $L_{\text{BB}}$ ) is near resonance, and the frequency of the free-bound laser ( $L_{\text{FB}}$ ) is scanned, Autler-Townes splitting of the PA resonance is observed. This splitting is equivalent to the generalized Rabi frequency of the bound-bound transition

$$\Omega'_{vv'} = \sqrt{(\omega - \omega_0)^2 + \Omega_{vv'}^2}, \quad (1)$$

where  $\omega$  is the frequency of  $L_{\text{BB}}$ ,  $\omega_0$  corresponds to the bound-bound resonance, and  $\Omega_{vv'}$  is the Rabi frequency. Near the dissociation limit,  $\Omega_{vv'}$  is directly related to the dimensionless FCF  $f_{vv'} = |\langle v'|v \rangle|^2$ , since  $\Omega_{vv'} = \Omega_a \sqrt{2f_{vv'}}\alpha$ , where  $\alpha^2 = 1/3$  is the rotational line strength for  $(J, J') = (0, 1)$  transitions, and the atomic Rabi frequency is  $\Omega_a = \Gamma_a \sqrt{s/2}$  in terms of the atomic spontaneous decay rate  $\Gamma_a$  and saturation parameter  $s$ .

Different  $(v, v')$  pairs yield complementary information on FCFs, and the details will be presented in a future publication. The pairs relevant to this work are  $(-2, -5)$  and  $(-3, -6)$ . The corresponding FCFs were calculated to be  $0.8(1)$ , indicating a particularly strong coupling between the levels. Figure 2 (a) shows the Autler-Townes peak positions for  $(v, v') = (-2, -5)$  at various frequencies of  $L_{\text{BB}}$ . The difference between the

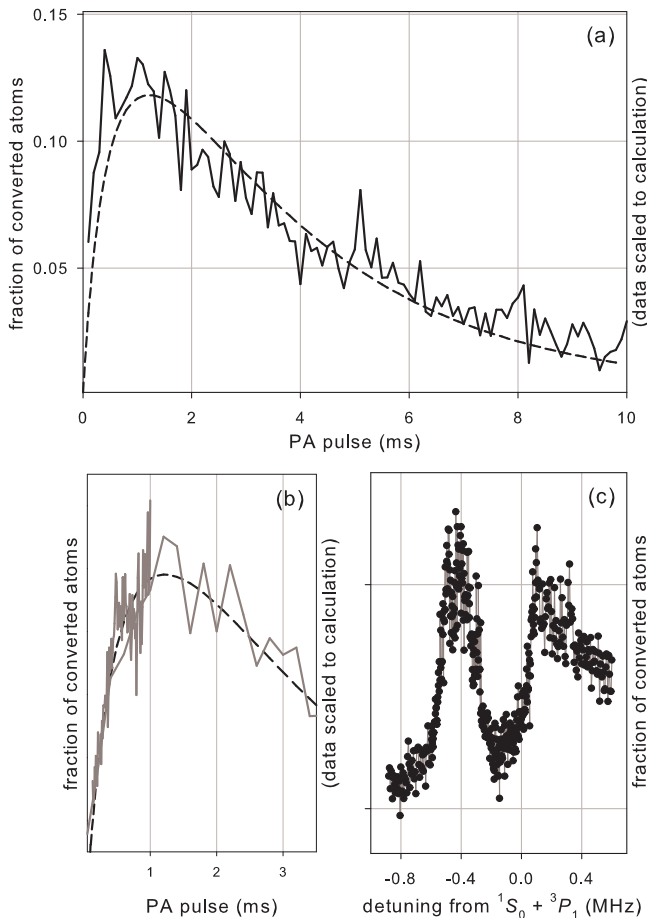


FIG. 3: (a) Solid line: fraction of the atom cloud detected after a molecule producing PA pulse followed by an atom clearing pulse and an atom recovery pulse. The data is scaled by an arbitrary factor, since the absolute efficiency of the atom recovery pulse is not fully known (see text); the lowest bound on the peak recovery fraction is  $\sim 2\%$ . Dashed line: calculated fraction of the atom cloud converted to  $v = -2$  molecules after the PA pulse. The curve parameters were measured independently, with the exception of the molecule lifetime, which was fixed at  $\sim 3$  ms to best match the data. (b) Same curve as in (a), with denser data in the first ms. (c) Fraction of the atom cloud detected after a 1 ms PA pulse followed by the atom clearing and atom recovery pulses, as a function of the  $L_{BB}$  frequency. The peak corresponds to the bound-bound transition from  $v = -2$  to  $v' = -1$ . Although the coupling of  $v = -2$  to the  $^1S_0 + ^3P_1$  thermal continuum is weaker than to  $v' = -1$ , at the high saturation intensity used here atoms are also recovered via the continuum, which is only 0.4 MHz away from  $v' = -1$ .

two curve branches is  $\Omega'_{(-2,-5)}$ , and is fitted to eq. (1). The FCF is found to be  $f_{(-2,-5)} = 1.1$ , which is consistent with 0.8(1) if the  $27 \mu\text{m}$  PA laser beam waist measurement has an error of just 15%. In contrast, Fig. 2 (b) shows the Autler-Townes peak positions and fit for  $(v, v') = (-3, -4)$ . With  $60\times$  more  $L_{BB}$  power, the

splitting is  $4.4\times$  smaller, leading to the experimentally determined ratio  $f_{(-3,-4)}/f_{(-2,-5)} = 0.9 \times 10^{-3}$ . This agrees well with the calculated ratio of  $1.1 \times 10^{-3}$ . While the  $(v, v') = (-3, -6)$  pair was not used in this work, our measurements have confirmed that its FCF is also near unity. Note that the fits such as shown in Fig. 2 yield the binding energies for  $v = -2$  and  $v = -3$  levels ( $J = 0$ ) as  $1,400.1(2) h \times \text{MHz}$  and  $5,110.6(1) h \times \text{MHz}$ , which agree with our calculations to 1.3% and 0.3%.

The FCFs between weakly bound vibrational levels were computed from adiabatic single-channel potentials fitted to high resolution Fourier transform spectra of Refs. [28, 29]. They were also calculated in Refs. [25, 26] by describing the rovibrational dynamics in the excited electronic states by a coupled multichannel fully-nonadiabatic Hamiltonian. The large calculated value of  $f_{(-2,-5)} = 0.8(1)$  is surprising at first glance since the wave function of  $v' = -5$  shows 38 oscillations, while the wave function of  $v = -2$  shows 61. However, according to the Franck-Condon principle [31], molecular transitions most readily occur between rovibrational levels of two different electronic states with classical turning points nearly the same. In the adiabatic picture the classical turning points of  $v' = -5$  and  $v = -2$  are very close, with their respective inner points at 7.1 and 7.5  $a_0$  and outer points at 47.1 and 50.0  $a_0$ . This near-coincidence explains the exceptionally large overlap between the two wave functions at large interatomic distances, as plotted in Fig. 1 (b). A similarly large overlap is predicted for  $v' = -6$  and  $v = -3$ , with the respective outer turning points at 40.5 and 40.1  $a_0$ .

The  $\text{Sr}_2$  molecule formation relies on one-photon PA into  $v' = -5$  followed by spontaneous decay into  $v = -2$ . The PA induced atom density loss from the lattice is described by  $\dot{n}_a = -2Kn_a^2$ , where  $K$  is the two-body loss rate and we have neglected the finite lifetime of the trapped atoms ( $\sim 10$  s). Thus  $n_a(t) = n_0/(1 + 2Kn_0t)$ , where  $n_0$  is the initial atom density. Hence the time evolution of the molecule density is approximately given by  $\dot{n}_m \approx 0.3f_{vv'}Kn_a^2 - n_m/\tau_c$ , where  $\tau_c = (n_0\gamma_c)^{-1}$  is the lifetime parameter for the created molecules assuming similar rates for molecule-atom and molecule-molecule collisional losses, and the 0.3 factor results from the spontaneous decay branching ratio from  $J' = 1$  to  $J = 0$  [32]. (Note that with a simple repumping scheme out of  $J = 2$ , an atom-molecule conversion efficiency of  $\sim 80\%$  is expected; without repumping, it is limited to  $\sim 25\%$ .) Therefore, the created molecule density as a fraction of  $n_0$  can be expressed as

$$\frac{d}{dt} \left( \frac{n_m}{n_0} \right) = \frac{b}{(1 + at)^2} - c \left( \frac{n_m}{n_0} \right). \quad (2)$$

For PA to  $v' = -5$ , the rates  $a = 2Kn_0$  (and therefore  $b = 0.3f_{vv'}Kn_0$ ) were determined by measuring atom loss as a function of the  $L_{FB}$  pulse length. At the  $L_{FB}$  power of 3.2 mW, we find  $a = 1,680/\text{s}$  and  $b = 220/\text{s}$ .

The loss rate also has to be measured; for the dominating molecule-atom collisions it can be estimated as  $c \approx 2hn_0R_6/\mu \sim 200/\text{s}$  [33] for our densities  $n_0 \sim 2 \times 10^{12}/\text{cm}^3$ , where  $\mu$  is the molecule-atom reduced mass; the van der Waals length  $R_6 = 0.5(2\mu C_6/\hbar^2)^{1/4} \approx 5.0$  nm, where  $\hbar = h/(2\pi)$  and  $C_6$  is the relevant dispersion coefficient. This  $\sim 5$  ms estimated collisional lifetime requires forming molecules on the ms time scale. While it requires relatively large intensities of  $L_{\text{FB}}$ , the undesirable photon scattering by the atomic transition is suppressed due to the narrow line. The numerical solution ( $2n_m/n_0$ ) to eq. (2) is plotted in Fig. 3 (a) for various PA pulse durations. As expected, for a sufficiently large PA rate  $a$ , the number of photoassociated atoms first rapidly grows, then gradually falls as the production slows relative to collisional loss.

After the PA pulse is applied to the atoms, they are exposed to a clearing pulse (on the strong  $^1S_0 - ^1P_1$  atomic transition at 461 nm) of the 0.1 ms minimum duration needed to remove the non-photoassociated atoms to below the background level. Then a 0.1 ms atom recovery pulse is applied to the molecules created in  $v = -2$ . This pulse is resonant with  $(v, v') = (-2, -1)$ ; the calculated  $f_{(-2, -1)} = 1.4 \times 10^{-5}$ . As discussed earlier,  $v' = -1$  has an exceptionally strong coupling to the free atom state:  $l_{\text{opt}} \sim 8 \times 10^5 a_0/(\text{W}/\text{cm}^2)$  from calculations and  $\sim 4 \times 10^5 a_0/(\text{W}/\text{cm}^2)$  from previous measurements [15]. Due to the small binding energy and large  $l_{\text{opt}}$ , at least  $\sim 50\%$  of the  $v' = -1$  molecules can be expected to spontaneously decay into ground state atoms that get recaptured in the optical lattice [27, 34].

Figure 3 (a, b) shows the result of the  $\text{Sr}_2$  electronic ground state molecule creation followed by conversion of the molecules back to atoms. An overall scaling factor has been applied to the data, since the efficiency of the recovery pulse is not yet fully known. The expected curve is obtained from eq. (2), with the molecule lifetime chosen to best match the data. This results in  $c \sim 380/\text{s}$ , or a lifetime of  $\sim 3$  ms of the  $v = -2$  molecules in the lattice. The calculated curve is not scaled, and predicts that at the given  $L_{\text{FB}}$  power, 12% of the atoms should be converted to  $\text{Sr}_2$  at optimal PA pulse lengths of 1 ms, roughly half the maximum possible fraction (without repumping). The actual fraction of recovered atoms is 1%, corresponding to a conversion of 2% of the atoms into molecules, assuming the maximum expected efficiency of the recovery pulse. Given this uncertainty, we conclude that we create  $4(3) \times 10^4$  molecules with the 1 ms PA pulse. We project that as a three-dimensional optical lattice is imposed on the atoms after the 1 ms PA pulse and the atom clearing pulse are applied, the molecules can be confined on time scales exceeding 1 s [10, 35].

Atom recovery via the least-bound excited molecular level is confirmed by choosing the optimal 1 ms molecule producing pulse duration, and measuring the recovered atom fraction as a function of the  $L_{\text{BB}}$  frequency, as

shown in Fig. 3 (c). The peak corresponds to the bound-bound transition from  $v = -2$  to  $v' = -1$ . Although the coupling of  $v = -2$  to the electronically excited thermal continuum is weaker than to  $v' = -1$ , at the high saturation intensity used here the atoms can also be recovered via the continuum, which is 0.4 MHz blue-detuned from the molecular line.

In conclusion, we have produced stable ultracold  $\text{Sr}_2$  molecules in the electronic ground state that are bound by  $0.05 \text{ cm}^{-1}$ . Our technique is the first step of a two-step projected sequence for achieving large samples of ultracold  $\text{Sr}_2$  in the absolute ground quantum state. This has immediate applications in precise time and frequency metrology, studies of fundamental constant variations, and investigations of chemical reactions at ultra low kinetic energies and highly non-thermal internal state distributions. The simple all-optical molecule creation scheme relies on a large wave function overlap between a pair of electronically excited and ground rovibrational levels that is characteristic of the alkaline earth atom system. The entire experimental trajectory ending in the  $\mu\text{K}$  molecule sample takes only 0.25 s. The atom recovery scheme, demonstrating the creation of the molecules, relies on one-photon excitation to the least-bound vibrational level near the intercombination line dissociation limit. This level can be resolved due to the narrow optical line width, and has an unusually large coupling to the thermal continuum of the ground electronic state. To achieve the goals of this work, we have performed one- and two-photon spectroscopic studies of  $\text{Sr}_2$ . *Note* that related results are being reported in a system of  $^{84}\text{Sr}$  in a Mott insulator state [36].

We acknowledge invaluable contributions to theoretical studies of our system by R. Moszynski, C. Koch, and W. Skomorowski. We also thank P. Julienne for many fruitful discussions, and K. Bega for contributions in the earlier stages of the experiment. This work was partially supported by the ARO and the AFOSR.

---

\* Electronic address: tz@phys.columbia.edu

- [1] L. D. Carr, D. DeMille, R. V. Krems, and J. Ye, **11**, 055049 (2009).
- [2] A. Micheli, G. K. Brennen, and P. Zoller, *Nature Phys.* **2**, 341 (2006).
- [3] S. Ospelkaus, K.-K. Ni, D. Wang, M. H. G. de Miranda, B. Neyenhuis, G. Quémener, P. S. Julienne, J. L. Bohn, D. S. Jin, and J. Ye, *Science* **327**, 853 (2010).
- [4] D. DeMille, *Phys. Rev. Lett.* **88**, 067901 (2002).
- [5] D. DeMille, S. Sainis, J. Sage, T. Bergeman, S. Kotochigova, and E. Tiesinga, *Phys. Rev. Lett.* **100**, 043202 (2008).
- [6] T. Zelevinsky, S. Kotochigova, and J. Ye, *Phys. Rev. Lett.* **100**, 043201 (2008).
- [7] E. S. Shuman, J. F. Barry, and D. DeMille, *Nature* **467**, 820 (2010).

- [8] J. M. Sage, S. Sainis, T. Bergeman, and D. DeMille, *Phys. Rev. Lett.* **94**, 203001 (2005).
- [9] T. Rom, T. Best, O. Mandel, A. Widera, M. Greiner, T. W. Hänsch, and I. Bloch, *Phys. Rev. Lett.* **93**, 073002 (2004).
- [10] J. G. Danzl, M. J. Mark, E. Haller, M. Gustavsson, R. Hart, J. Aldegunde, J. M. Hutson, and H.-C. Nägerl, *Nature Phys.* **6**, 265 (2010).
- [11] F. Lang, K. Winkler, C. Strauss, R. Grimm, and J. H. Denschlag, *Phys. Rev. Lett.* **101**, 133005 (2008).
- [12] K.-K. Ni, S. Ospelkaus, M. H. G. de Miranda, A. Pe'er, B. Neyenhuis, J. J. Zirbel, S. Kotochigova, P. S. Julienne, D. S. Jin, and J. Ye, *Science* **322**, 231 (2008).
- [13] G. Barontini, C. Weber, F. Rabatti, J. Catani, G. Thalhammer, M. Inguscio, and F. Minardi, *Phys. Rev. Lett.* **103**, 043201 (2009).
- [14] C. Chin, R. Grimm, P. Julienne, and E. Tiesinga, *Rev. Mod. Phys.* **82**, 1225 (2010).
- [15] T. Zelevinsky, M. Boyd, A. Ludlow, T. Ido, J. Ye, R. Ciuryło, P. Naidon, and P. Julienne, *Phys. Rev. Lett.* **96**, 203201 (2006).
- [16] H. Katori, T. Ido, Y. Isoda, and M. Kuwato-Gonokami, *Phys. Rev. Lett.* **82**, 1116 (1999).
- [17] K. M. Jones, E. Tiesinga, P. D. Lett, and P. S. Julienne, *Rev. Mod. Phys.* **78**, 483 (2006).
- [18] Y. N. M. de Escobar, P. G. Mickelson, P. Pellegrini, S. B. Nagel, A. Traverso, M. Yan, R. Côté, and T. C. Killian, *Phys. Rev. A* **78**, 062708 (2008).
- [19] S. Blatt, T. L. Nicholson, B. J. Bloom, J. R. Williams, J. W. Thomsen, P. S. Julienne, and J. Ye, *Phys. Rev. Lett.* **107**, 073202 (2011).
- [20] Y. Takasu, Y. Saito, Y. Takahashi, M. Borkowski, R. Ciuryło, and P. S. Julienne, *Phys. Rev. Lett.* **108**, 173002 (2012).
- [21] H. Hara, Y. Takasu, Y. Yamaoka, J. M. Doyle, and Y. Takahashi, *Phys. Rev. Lett.* **106**, 205304 (2011).
- [22] A. H. Hansen, A. Khramov, W. H. Dowd, A. O. Jamison, V. V. Ivanov, and S. Gupta, *Phys. Rev. A* **84**, 011606(R) (2011).
- [23] N. Nemitz, F. Baumer, F. Münchow, S. Tassy, and A. Görlitz, *Phys. Rev. A* **79**, 061403(R) (2009).
- [24] M. Tomza, F. Pawłowski, M. Jeziorska, C. P. Koch, and R. Moszynski, *Phys. Chem. Chem. Phys.* **13**, 42 (2011).
- [25] W. Skomorowski, R. Moszynski, and C. P. Koch, *Phys. Rev. A* **85**, 043414 (2012).
- [26] W. Skomorowski, F. Pawłowski, C. P. Koch, and R. Moszynski, *J. Chem. Phys.* **136**, 194306 (2012).
- [27] R. Moszynski, private communication.
- [28] A. Stein, H. Knöckel, and E. Tiemann, *Eur. Phys. J. D* **57**, 171 (2010).
- [29] A. Stein, H. Knöckel, and E. Tiemann, *Phys. Rev. A* **78**, 042508 (2008).
- [30] T. Ido and H. Katori, *Phys. Rev. Lett.* **91**, 053001 (2003).
- [31] E. U. Condon, *Phys. Rev.* **32**, 858 (1928).
- [32] S. Kotochigova, T. Zelevinsky, and J. Ye, *Phys. Rev. A* **79**, 012504 (2009).
- [33] P. S. Julienne, T. M. Hanna, and Z. Idziaszek, *Phys. Chem. Chem. Phys.* **13**, 19114 (2011).
- [34] P. Julienne, private communication.
- [35] A. Chotia, B. Neyenhuis, S. A. Moses, B. Yan, J. P. Covey, M. Foss-Feig, A. M. Rey, D. S. Jin, and J. Ye, *Phys. Rev. Lett.* **108**, 080405 (2012).
- [36] S. Stellmer, B. Pasquiou, R. Grimm, and F. Schreck, arXiv:1205.4505.